Journal of Power Sources 193 (2009) 462–469

Contents lists available at ScienceDirect

Journal of Power Sources

journal homepage: www.elsevier.com/locate/jpowsour

A proper amount of carbon nanotubes for improving the performance of Pt–Ru/C catalysts for methanol electro-oxidation

Ching-Fa Chi, Ming-Chang Yang, Hung-Shan Weng*

Department of Chemical Engineering, National Cheng Kung University, Tainan 701, Taiwan

ARTICLE INFO

Article history:
Received 19 December 2008
Received in revised form 18 March 2009
Accepted 10 April 2009
Available online 18 May 2009

Keywords:
Methanol electro-oxidation
Pt–Ru catalysts
Carbon nanotubes
Mesoporous carbon
Direct methanol fuel cell

ABSTRACT

This study aims to improve the performance of the anode catalyst in a direct methanol fuel cell by using carbon black (XC) and mesoporous carbon (MC) as supporting materials for preparing Pt–Ru/XC and Pt–Ru/MC catalysts. This study investigates the effect of adding different amounts of bare carbon nanotubes (CNTs) or carbon nanotubes impregnated with Pt and Ru (abbreviated as Pt–Ru/CNT, containing 10 wt.% Pt and Ru) to the prepared catalysts. Experimental results reveal that 10 wt.% Pt–Ru/C with carbon black and mesoporous carbon prepared by the multiple impregnation method had smaller Pt–Ru grain sizes and a better dispersion or carbon supports due to low precursor concentrations in each impregnation. These, in turn, achieved better electro-catalytic performance for methanol oxidation. Adding CNTs or Pt–Ru/CNT to Pt–Ru/XC and Pt–Ru/MC obviously improves their electro-catalytic characteristics. The appropriate amounts of bare CNT and Pt–Ru/CNT added to Pt–Ru/XC and Pt–Ru/MC catalysts are 5% and 20%, respectively. The resulting catalysts (both containing 10 wt.% Pt and Ru) produce activities similar to those of the E-TEK Pt–Ru/C catalyst containing 20 wt.% Pt and Ru.

1. Introduction

A fuel cell is a device which can transfer chemical energy from fuel into electric energy. With the goal of attaining practical power levels and reducing manufacturing costs, particularly in small power generation and portable systems, recent research and industrial initiatives have focused their work on direct methanol fuel cells (DMFCs). This type of fuel cell is more convenient than a proton exchange membrane fuel cell (PEMFC) with hydrogen fuel [1–3]. However, it still needs to overcome problems such as (1) insufficient electro-catalytic activity of the anode catalyst for methanol oxidation; (2) catalyst deactivation due to methanol oxidation on platinum catalysts that generates intermediates such as CO that can be adsorbed on the Pt surface; (3) "crossover" caused by methanol penetrating through the anode to the cathode membrane [3,4]. Preparing a low Pt-loaded anode catalyst with high electro-catalytic activity and stability for future methanol oxidation is an important goal for commercialization.

Adding a secondary metal (M) to form a Pt–M binary alloy can enhance the catalyst's CO tolerance [3,5,6]. Ruthenium (Ru), which forms the Pt–Ru alloy, outperforms several other secondary metals for hydrogen electro-oxidation in the presence of CO [7], and also offers better methanol electro-oxidation [3].

Reducing the Pt–Ru grain size is very important for enhancing the electro-catalytic activity of PEMFCs and DMFCs and reducing their cost. The result is a larger active surface area of Pt–Ru grains on the Pt–Ru/C catalyst [8], achieved by selecting the appropriate carbon support and a suitable preparation method. Previous studies propose various fabrication methods for low-Pt-loading electro-catalysts [9,10] and discuss the role of carbon in fuel cells [11].

Carbon materials usually have a high surface area to disperse metal grains, and their high conductivity transfers electrons generated from electrochemical reactions taking place on the anode. Therefore, the metal particles are often supported on carbon black (such as Vulcan XC-72) or other carbons with a high surface area. Several researchers have successfully synthesized mesoporous carbon materials with an ordered pore structure using different methods [12–14]. These synthesized mesoporous carbons usually have a regular array of uniform pores and high specific surface area that promotes the fuel diffusion rate into pores, and hence enhances the reaction rate.

Dicks [11] points out that carbon nanotube (CNT) development and nanotechnology has opened up possibilities for using new materials in low-temperature fuel cells. Carbon nanotubes can be used for catalyst supports due to their graphitic structure and high electrical conductivity [15,16] though they still have less surface area than other porous carbons. Yang et al. [17] used carbon nanotubes as Pt–Ru catalyst supports for methanol electro-oxidation. He et al. [18,19] deposited Pt and Pt–Ru nanoparticles on a CNT and graphite electrode prepared by growing CNTs directly on a graphite

* Corresponding author. Fax: +886 6 2344496.
E-mail address: z5408008@email.ncku.edu.tw (H.-S. Weng).

0378-7753/$ – see front matter © 2009 Elsevier B.V. All rights reserved.
doi:10.1016/j.jpowsour.2009.04.079

disk for methanol electro-oxidation. Wang et al. [20] grew carbon nanotubes directly on a carbon cloth and used it for methanol electro-oxidation. Carbon nanotubes have also been used as supports to prepare Pt–Ru catalysts for PEMFCs and DMFCs [21–23]. However, researchers have not reported the effect of CNTs on Pt–Ru catalyst performance.

This study prepares Pt–Ru/C catalysts containing 10 wt.% Pt with an atomic ratio of Pt/Ru = 1 using the incipient wetness impregnation method. Both carbon black and mesoporous carbon are used as supports. This study also adopts the multiple impregnation method to improve carbon electro-catalytic activities when the carbon supports are loaded with Pt and Ru. The prepared Pt–Ru/C catalysts are characterized by N_2 desorption, XRD, SEM, TEM and EDS. A three-electrode cell measures their electro-catalytic activities for methanol oxidation after their fabrication on a catalytic electrode. Experiments in this study add carbon nanotubes, either bare or loaded with Pt and Ru, to the Pt–Ru/C catalysts to observe the promoting effect. Results show the optimal added amounts.

2. Experimental

2.1. Preparation of Pt–Ru/C catalysts

The experiment in this study used three kinds of carbon materials, XC (XC-72, Cabolt), MC (Supplied by Professor H.-P. Lin, Department of Chemistry, National Cheng Kung University, Taiwan) and CNTs (Aldrich) as supports for Pt–Ru/C catalysts. The carbon supports were boiled in a 6 M HNO_3 solution (Scharlau) for 2 h in a reflux system before being loaded with Pt and Ru. After cooling and washing with deionized water until pH 6, the carbon materials were dried at 120 °C to remove water before utilizing the incipient wetness impregnation method for catalyst preparation. In impregnation, 0.245 g of carbon material were mixed with an appropriate amount of solution containing H_2PtCl_6 (Aldrich) and equimolar $RuCl_3$ (Acros). Then 0.5 mL of 5 wt.% Nafion solution (Aldrich) was added drop by drop for two purposes: dispersing the metal salts and enhancing proton transport capability. This solution was then dried by stirring in atmosphere for 4–5 h in a dry box at 80 °C for 5 h. The powder was ground slightly before adding 10 mL of methanol (or methanol containing 0.018 g $NaBH_4$) as a reducing agent [9]. The resulting slurry was refluxed at 70 °C for 5 h. The mixture was then cooled, filtrated, washed with deionized water to remove chloride ions, and dried at 80 °C for 4 h. The same experimental process was repeated when applying the multiple impregnation method to prepare Pt–Ru/C catalysts for the same total metal loading. However, the metal salt concentration was reduced for the multiple impregnation experiment. For example, in double impregnation, each impregnation uses only half the concentration of Pt and Ru precursors for single impregnation.

The prepared catalysts are designated as a "support-reducing agent (n)". The supports include XC, MC, and CNT. The experiment uses methanol (abbreviated to "M") and methanol containing $NaBH_4$ (denoted as "N") as reducing agents. The numbers in parentheses denote the number of impregnation. For example, XC-N(1) represents the catalyst prepared using methanol containing $NaBH_4$ as a reducing agent after a single impregnation on XC. An additional number after the parenthesis indicates the weight percentage of the loaded Pt and Ru when CNTs are used as the support.

2.2. Addition of carbon nanotubes

In a previous study in our laboratory, XC, CNTs and their mixture were employed as the supports of Pt–Ru catalysts. The performance of Pt–Ru/XC-CNT for methanol electro-oxidation was found far better than that of Pt–Ru/XC catalyst, and the addition of Pt–Ru/CNT also enhanced the performance of Pt–Ru/XC catalyst (see Appendix A). To further investigate the effect of CNTs on the performance of Pt–Ru/C catalysts for methanol electro-oxidation, this study carried out a set of preliminary experiments by adding 0, 25, 50 and 75 wt.% of CNTs to Pt–Ru/XC catalysts to fabricate the catalytic electrodes. Results show that the optimum might exist between 0 and 25 wt.%, so the experiment added 0, 5, 10, 15, 20 and 25 wt.% of CNTs or Pt–Ru/CNT (containing 10 wt.% Pt and Ru) to Pt–Ru/XC and Pt–Ru/MC and again searched for the optimal added amounts.

2.3. Physical characterization

This study used the Brunauer–Emmett–Teller (BET) method to determine the specific surface area of carbon materials and Pt–Ru/C catalysts using a nitrogen adsorption/desorption apparatus (Micrometritics ASAP-2010). The BJH desorption method determines the pore size distributions of all samples. A diffractometer (Rigaku D/MAX) obtained the X-ray diffraction (XRD) patterns of catalysts using Cu Kα source (λ = 0.15405 nm) operated at 40 kV, 30 mA, and scanning rate was 4° min^{-1} for 2θ values between 10° and 90°. A scanning electron microscope (SEM, JOEL JSM-6700) and transmission electron microscope (TEM, Philip CM200) revealed the surface morphology of carbon supports and catalysts as well as metal grain sizes on the as-prepared catalysts.

2.4. Electrochemical measurements

A potentiostat (EG&G, Model 273A) measured the signal from a beaker-type device with a three-electrode cell consisting of a working electrode, a Pt wire counter electrode, and a saturated calomel (SCE) reference electrode. The following procedure was used to prepare the working electrode. The procedure first mixed the as-prepared catalyst with an appropriate amount of Nafion solution (5 wt.%, Aldrich) by stirring at room temperature. Then the slurry was brushed a carbon cloth (Taiwan Carbon Technology AW 1114, 6 cm^2) and dried at 80 °C to remove excess water. Finally, this catalyst layer was fixed on a current collector of Pt wire between two Teflon plates. The counter electrode, 5 cm in length and 0.05 cm in diameter, was located 5 cm away from the working electrode. In a testing experiment, the platinum wire counter electrode was replaced by a platinum sheet 3 cm × 4 cm. The results showed that no difference in the polarization curves was observed with these two types of counter electrodes. All electrochemical measurements were taken at 30–75 °C with linear sweep voltammetry (LSV) at a scanning rate of 1 mV s^{-1} in 0.5 M H_2SO_4 (Fluka) solution containing 1 M CH_3OH (ECHO, HPLC grade). The experiment repeated each measurement three times, observing approximately 5% deviation.

3. Results and discussion

3.1. N_2 adsorption/desorption analyses

The experiment above determined the textual properties of supports and catalysts using N_2-BET measurements. The specific surface areas of the nitric acid-treated carbon black (XC) and mesoporous carbon (MC) are 220.4 and 607.7 m^2 g^{-1}, respectively. Fig. 1(a) and (b) shows the N_2 adsorption–desorption isotherms and pore size distributions of the two carbon materials, respectively. The pore size distributions of MC and XC are mainly in the ranges of 2–4 nm and 30–80 nm, respectively. Compared with XC, the MC pore volume is small and its pore size distribution is sharp and narrow. The MC pore volume is mainly attributed to internal pores (mesopores) in the MC crystallites while that of XC results from pores formed by the carbon black stack. Using these two carbon powders as catalyst supports for Pt–Ru/C shows that the pore

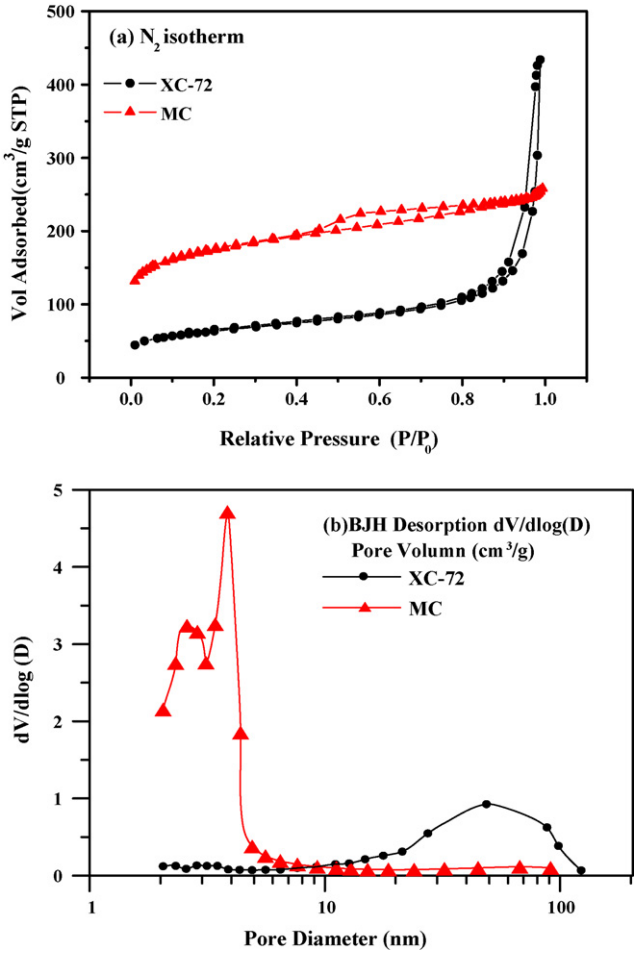

Fig. 1. (a) N_2 adsorption/desorption isotherm and (b) pore size distribution of XC-72 and MC without loaded metals.

characteristics of MC and XC affect grain formation and size of active metals.

The BJH desorption method obtains the pore volumes of carbon supports (XC and MC) and Pt–Ru/C prepared with various impregnations. Most MC pores are smaller than 10 nm, while XC pores are generally larger than 10 nm. This study discusses the effect of pore size on catalysts based on two categories, namely, mesopores (<10 nm) and macropores (>10 nm). Table 1 shows the total pore volumes and mesopore and macropore volumes for supports and catalysts. Catalysts prepared with methanol containing $NaBH_4$ as the reducing agent show smaller pore volumes than those without $NaBH_4$. This result might be attributed to the fact that some Pt–Ru particles, prepared with $NaBH_4$, are smaller than the mesopores of carbon supports and can more easily reside in the pores (see Section 3.4 and Table 2). The volume difference between the mesopores (<10 nm) of XC-M(1) and XC-N(1) is far smaller than that of MC-M(1) and MC-N(1). This volume difference is because MC pores are mainly located in the mesopore range (<10 nm), close to the Pt–Ru particle sizes.

For catalysts prepared using the methanol containing $NaBH_4$ as the reducing agent, pore volume decreases as the impregnation time increases. The reason cited above may also apply to this pore volume difference. The precursor concentration decreases as number of impregnation increases, creating smaller Pt–Ru particles which can easily reside in the smaller pores and reduce the catalyst pore volume.

Table 1
Pore volumes ($cm^3\ g^{-1}$) of carbon supports and catalysts prepared.

Catalyst[a]	Total pore volume[b]	Volume of pores smaller than 10 nm	Volume of pores larger than 10 nm
XC	0.637	0.081	0.556
XC-M(1)	0.402	0.042	0.362
XC-N(1)	0.387	0.051	0.337
XC-N(2)	0.326	0.062	0.264
XC-N(3)	0.305	0.056	0.249
MC	0.256	0.216	0.040
MC-M(1)	0.246	0.206	0.040
MC-N(1)	0.203	0.168	0.035
MC-N(2)	0.187	0.153	0.037
MC-N(3)	0.184	0.145	0.039

[a] XC-M(1) and MC-M(1) represent the catalysts prepared using methanol without adding $NaBH_4$ as a reducing agent after single impregnation. XC-N(1) and MC-N(1) represent the catalysts prepared using methanol with adding $NaBH_4$ as a reducing agent after single impregnation. Number in parenthesis denotes the times of impregnation.
[b] Obtained by the BJH desorption method.

Table 2
Sizes of Pt–Ru grains on catalysts[a] and current densities induced.

Catalyst[b]	Grain size (from XRD)[c]	Grain size (from TEM)[d]	Current density[e] at 30 °C	Current density[e] at 75 °C
XC-M(1)	8.21	7.03	2.22	5.12
XC-N(1)	7.57	6.36	3.13	5.63
XC-N(2)	5.29	5.91	3.70	6.69
XC-N(3)	4.91	4.09	4.13	7.16
MC-M(1)	6.54	14.08	1.88	4.03
MC-N(1)	4.56	8.00	2.57	4.74
MC-N(2)	4.08	4.94	3.19	5.71
MC-N(3)	4.07	3.95	3.74	6.83
E-TEK[a]	4.40	5.95	4.61	7.47

[a] Except for the E-TEK catalyst containing 20 wt.% of Pt and Ru, all other catalysts contain only 10 wt.%.
[b] Refers to the designation explanation in Table 1 footnote.
[c] Calculated by Scherrer's equation (nm).
[d] Mean particle size from TEM (nm).
[e] mA mg^{-1}, at 0.6 V vs. SCE.

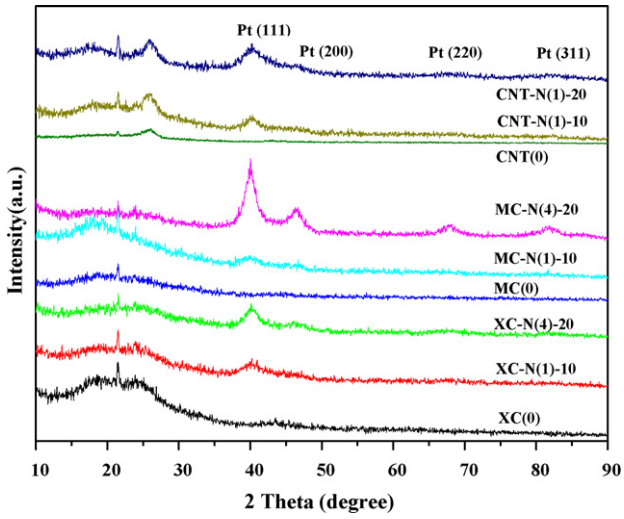

Fig. 2. XRD patterns of several supports and Pt–Ru/C catalysts prepared. Here, XC, MC, and CNT, respectively represent the carbon black, mesoporous carbon, and carbon nanotubes and catalysts prepared with XC, MC, and CNT as their supports. The numbers in parenthesis denote the times of impregnation, where 0 stands for no impregnation. All catalysts were loaded with 10 wt.% of Pt and Ru except for those labeled with "20," which contain 20 wt.% of Pt and Ru.

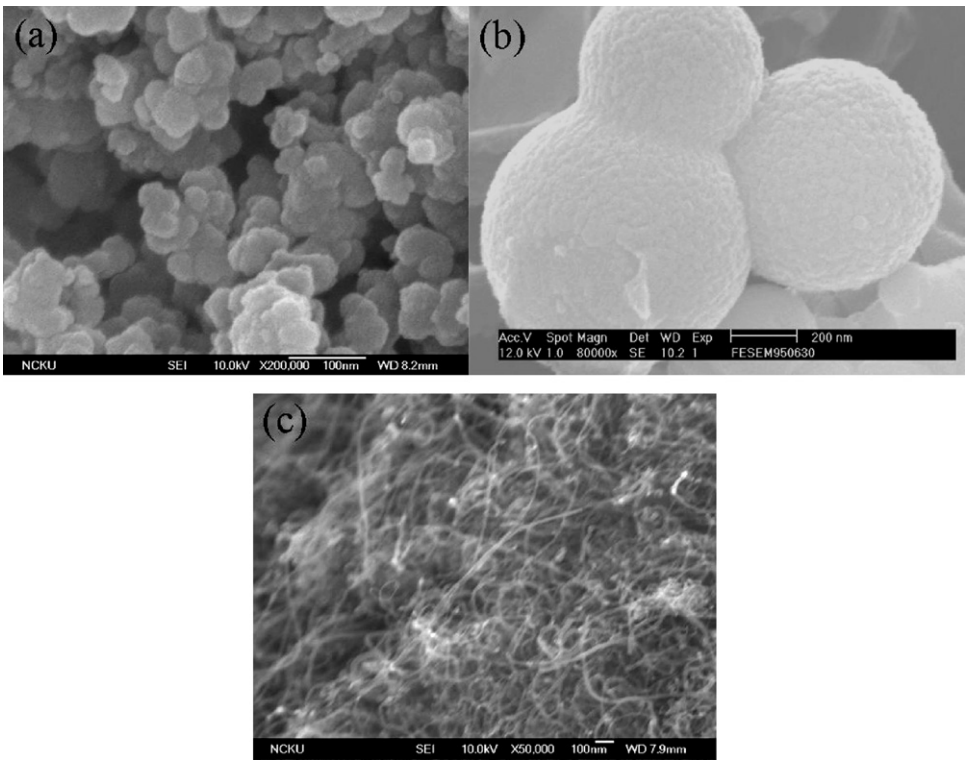

Fig. 3. SEM images of (a) XC, (b) MC, and (c) CNTs without Pt and Ru loaded.

3.2. XRD

The XRD pattern in Fig. 2 shows the f.c.c. Pt structure inferred from four characteristic peaks. The average Pt–Ru grain size of catalysts was obtained by Scherrer's equation. This study selects the most distinct peak, Pt (1 1 1) around $2\theta = 39.7^\circ$, to estimate the average Pt–Ru grain size, listed in Table 2.

3.3. SEM

Fig. 3 indicates that XC and MC are both spherical, with diameters of 20–30 nm and 400–600 nm, respectively, while CNTs look like seaweed with stems of 20–40 nm in diameter.

3.4. TEM

Fig. 4 shows that the Pt–Ru grains on carbon support prepared with methanol containing $NaBH_4$ as the reducing agent are visibly smaller than those without $NaBH_4$. Adding $NaBH_4$ to methanol enhances its reducing ability and raises the Pt–Ru nucleation rate, producing smaller metal grains. This study draws the Pt–Ru grain size distribution by measuring 250–300 grains in each TEM image. Table 2 lists the average grain sizes. The average grain sizes of the Pt–Ru/XC and Pt–Ru/MC catalysts decrease as number of impregnation increases. As mentioned above, the smaller size of the catalyst prepared via the multiple impregnation method could account for the lower precursor concentration in each impregnation.

3.5. EDS

Table 3 lists the Pt contents and molecular ratios of Pt/Ru in the prepared electro-catalysts. The Pt contents in all catalysts are slightly less than the nominated value (10 wt.%). This might be due to some Pt loss during impregnation. The molecular ratios of Pt/Ru in Pt–Ru/XC and Pt–Ru/MC are all greater than one, while some X in Pt–Ru/CNT are less than one. This implies a segregation of Pt and Ru on the Pt–Ru surface, and changing interaction between the Pt–Ru alloy based on the type of carbon supports.

3.6. Electrochemical measurements

Fig. 5 shows the current densities, based on catalyst weight ($mA\,mg^{-1}$) of the electrode with the as-prepared catalysts at 0.6 V vs. SCE for methanol oxidation with linear sweep voltammograms (LSV) at 30 and 75 °C. Table 2 also lists this data for analysis of the effect of Pt–Ru grain size. The reducing agent, the number of impregnations, and the type of carbon support all affect the induced current density. The current increases with the amount of $NaBH_4$ added into methanol, and with the number of impregnation times. The catalyst with smaller uniform Pt–Ru particles has a larger active surface area for catalyzing methanol oxidation, and hence exhibits higher electro-catalytic activity. TEM images and the data in Table 2 show that the catalyst prepared with the $NaBH_4$ methanol solution as the reducing agent and the multiple impregnation method produced higher activity because of its smaller Pt–Ru grain size.

Table 3
Pt contents and molecular ratios of Pt/Ru in Pt–Ru/C measured by EDS.

Catalyst[a]	Pt content (wt.%)[b]	Molecular ratio of Pt/Ru[c]
XC-N(1)	9.45	1.15
XC-N(2)	9.53	1.16
XC-N(3)	9.61	1.06
MC-N(1)	9.72	1.03
MC-N(2)	9.61	0.96
MC-N(3)	9.66	0.91
CNT-N(1)	9.11	0.91

[a] Refers to the designation explanation in Table 1 footnote.
[b] Nominal Pt content = 10 wt.%.
[c] Nominal molecular ratio of Pt/Ru = 1.

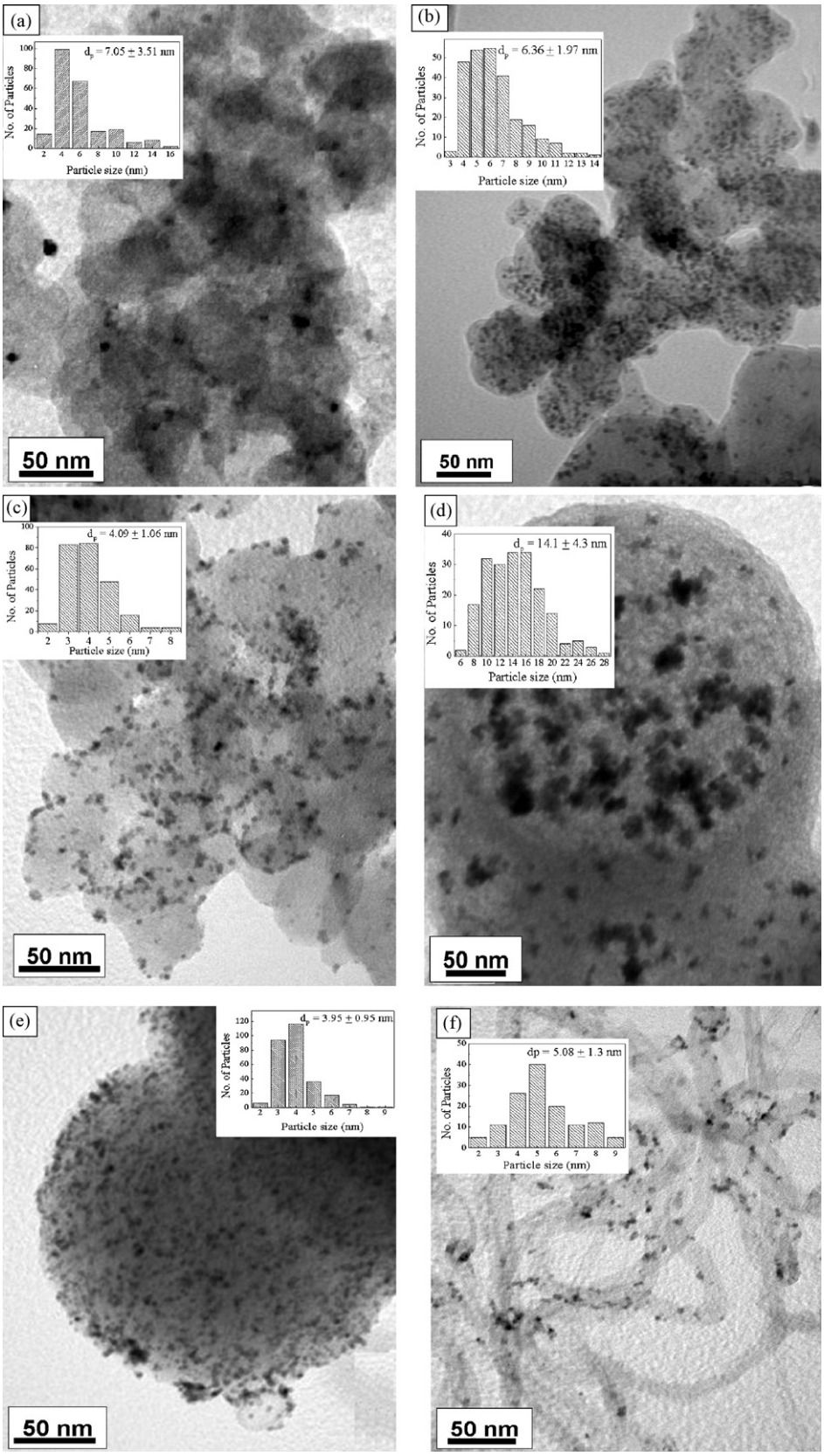

Fig. 4. TEM images of 10 wt.% Pt–Ru/C: (a) XC-M(1), (b) XC-N(1), (c) XC-N(3), (d) MC-N(1), (e) MC-N(3), and (f) CNT(N).

As for the effect of various carbon supports, the Pt–Ru catalysts supported by carbon black (XC) have higher electro-catalytic activities than those supported by mesoporous carbon (MC). This fact might be attributed to the electrical conductivities and pore size distributions of X. Carbon black has better electrical conductivity than mesoporous carbon unless the latter is graphitized at a high temperature. Although the surface area of carbon support is an important parameter for characterizing catalyst performance,

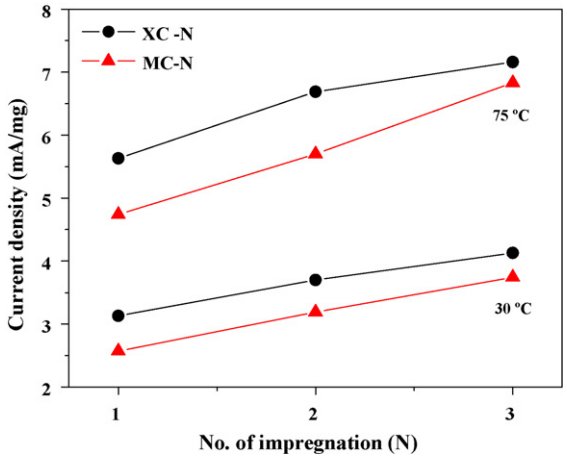

Fig. 5. Effect of the impregnation times on the electrochemical performance of electrodes with 10 wt.% Pt–Ru/C for methanol oxidation with LSV (0.6 V vs. SCE).

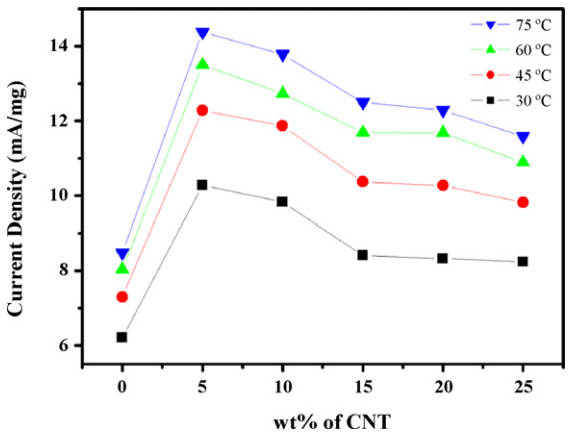

Fig. 7. Effect of the amount of bare CNTs added on electrode performance with Pt–Ru/XC for methanol electro-oxidation with LSV (0.6 V vs. SCE).

pore size distribution also plays an important role in loading metal nanoparticles onto the surface and diffusing reactant through the pores to access active sites. As Fig. 1 indicates, mesoporous carbon has smaller pores than carbon black, though the former has a greater surface area.

Fig. 6 shows the polarization curves of the prepared Pt–Ru/CNT catalysts and the commercial E-TEK 20 wt.% Pt–Ru/XC catalyst. The electro-catalytic activity of the Pt–Ru/CNT catalyst containing 10 wt.% of Pt and Ru is almost the same as that of the E-TEK 20 wt.% Pt–Ru/C catalyst. The Pt–Ru/CNT catalyst containing 20 wt.% of Pt and Ru has much higher X than the other three. This fact might be attributed to the high electrical conductivity of CNTs. This study added small amounts of bare CNTs and Pt–Ru/CNT to Pt–Ru/XC and Pt–Ru/MC catalysts to take advantage of CNT cost. The following investigation searches for the optimal added amounts to improve the electrochemical performance of catalysts.

In addition to Pt–Ru particle size, pore size distribution and conductivity of carbon materials, electro-catalyst performance might be affected by other factors such as the diameter and length of carbon nanotubes and spacing between carbon particles, and hence the resultant degree of mixing and extent of contact. The carbon supports in this study have varying shapes and sizes. The diameters of XC, MC, and CNTs are 20–30 nm, 400–600 nm and 3–10 nm, respectively (CNTs are about 0.1–10 μm in length). Adding larger amounts of CNT to XC and MC results in lower overall catalyst activity, as the XC and MC particles cannot contact each other due to CNT entanglement.

Figs. 7 and 8 show the results of adding bare CNTs and Pt–Ru/CNT (containing 10 wt.% Pt and Ru) to Pt–Ru/XC and Pt–Ru/MC, respectively. Adding bare CNTs to Pt–Ru/XC (or Pt–Ru/MC) uses the amount of Pt–Ru/XC or Pt–Ru/MC) in the catalyst. This in turn reduces the amount of Pt–Ru in the final catalyst mixture. For example, adding 5 wt.% of bare CNTs mean that the catalyst only uses 95 wt.% of Pt–Ru/XC (or Pt–Ru/MC). Note that Pt–Ru loading in the final Pt–Ru/C catalyst decreases after adding bare CNTs to Pt–Ru/XC and Pt–Ru/MC. However, the loading does not change after adding Pt–Ru/CNT to Pt–Ru/MC because the weight percentages of Pt and Ru in Pt–Ru/CNT are the same as those in Pt–Ru/MC.

Based on the current density comparisons at 0.6 V (vs. SCE) in Fig. 7, adding 5 wt.% of bare CNTs to Pt–Ru/XC produces the best performance for methanol electro-oxidation. The current density declines as the weight percentage of bare CNTs increases. This is probably because Pt loading decreases and these two carbon materials cannot contact well. When adding CNT to Pt–Ru/XC, the current density is higher than that without the addition, regardless of the percentage added. The optimal added amount is only 5 wt.% for 14.3 mA mg^{-1} at 75 °C.

Fig. 8 shows that when adding bare CNTs to Pt–Ru/MC, the current density increases as the weight percentage of bare

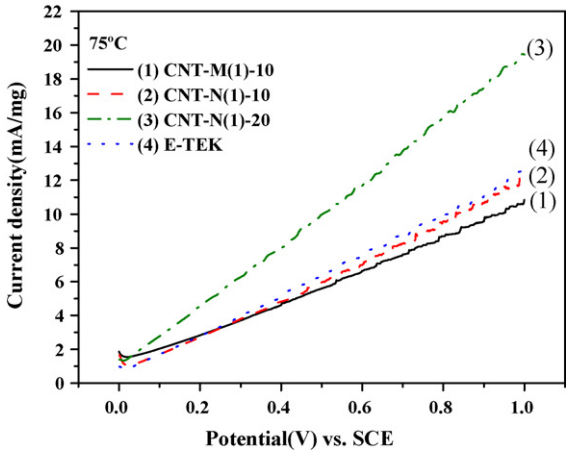

Fig. 6. LSV of electrode with Pt–Ru/CNT catalyst for methanol electro-oxidation at 75 °C with 1 mV s^{-1} scanning rate in half-cell containing 0.5 M H_2SO_4 and 1 M CH_3OH.

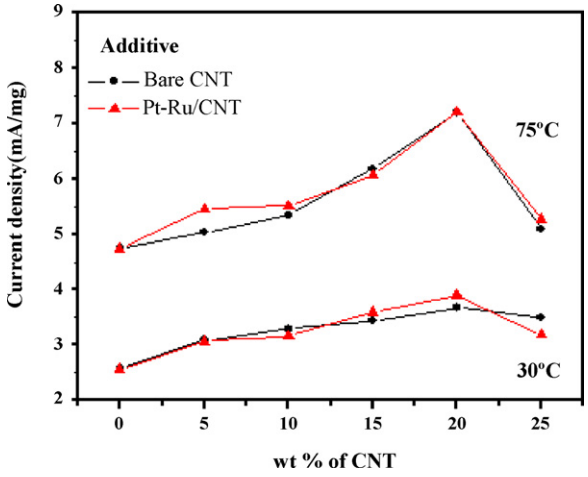

Fig. 8. Effect of the amount of bare CNTs and Pt–Ru/CNT (containing 10 wt.% Pt and Ru) added on the electrochemical performance of Pt–Ru/MC for methanol electro-oxidation with LSV (0.6 V vs. SCE).

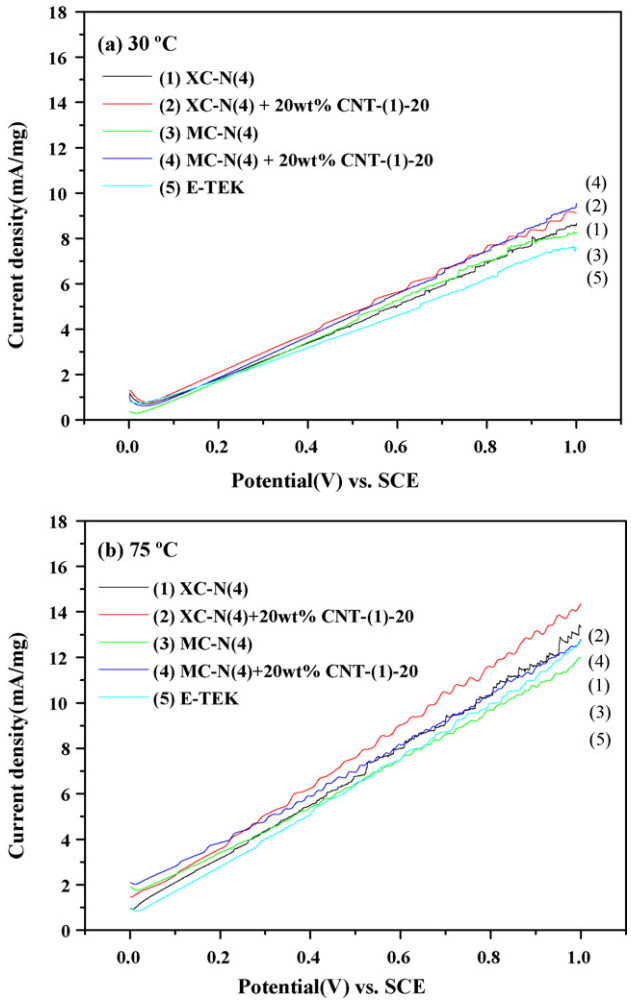

Fig. 9. Comparison of various electrodes for methanol electro-oxidation. The electrodes were prepared by adding 5 wt.% CNT(20) to 20 wt.% Pt–Ru/XC and Pt–Ru/MC prepared with quadruple impregnation. CNT(20) stands for the carbon nanotubes containing 20 wt.% Pt and Ru. All catalysts contained 20 wt.% Pt and Ru.

CNTs increases from 5 to 20 wt.%, with a maximum value of 7.19 mA mg^{-1} at 75 °C. Results indicate that the highest current density (7.19 mA mg^{-1}, 75 °C) occurs at 20 wt.% after adding Pt–Ru/CNT to Pt–Ru/MC. The difference in optimal added amounts for Pt–Ru/XC and Pt–Ru/MC catalysts may be due not only to electrical conductivity differences of XC and MC, but also to size differences. The size of MC is much larger than XC, and close to the length of CNT (0.1–10 um). Therefore, MC needs more CNTs as the mediate for MC particles to contact well with each other.

Both Pt–Ru/XC and Pt–Ru/MC catalysts with added optimal amounts of CNTs perform nearly the same as the E-TEK 20 wt.% Pt–Ru catalyst. However, the Pt and Ru loadings in the first two catalysts are only 10 and 5.81 wt.% (atomic ratio of Pt:Ru = 1:1), respectively, while the Pt and Ru in E-TEK are 20 and 13 wt.%. For further comparison, this research also prepared Pt–Ru/C catalysts with quadruple impregnation of 20 wt.% of Pt and Ru with XC and MC supports. This Pt–Ru/XC (or Pt–Ru/MC) was mixed with 20 wt.% of Pt–Ru/CNT (containing 20 wt.% of Pt and Ru) to fabricate catalyst electrodes. The resulting electrodes produce 10–20% more electro-catalytic activities than that of the E-TEK catalyst shown in Fig. 9.

4. Conclusions

The following conclusions can be drawn from the above discussion:

(1) Adding $NaBH_4$ to methanol as the reducing agent produces smaller Pt–Ru grains with a uniform dispersion on the carbon support. The result is higher electro-catalytic activity for methanol oxidation than with methanol alone.
(2) Under the same metal loading, catalysts prepared with the multiple impregnation method produce smaller Pt–Ru grains and hence exhibit higher electrochemical performance than catalysts prepared via single impregnation. Electro-catalytic activity increases with impregnation times.
(3) The Pt–Ru catalysts supported by carbon black show higher levels of electro-catalytic activity than those supported by mesoporous carbon due to higher electrical conductivity and appropriate pore size distribution in the former.
(4) Adding CNTs or Pt–Ru/CNT to Pt–Ru/XC and Pt–Ru/MC enhances the electro-catalytic activity of the catalyst electrode. An optimal added amount exists for each kind of catalyst. The electrochemical performances of these catalyst electrodes (containing only 10 wt.% Pt and 7 wt.% Ru) are nearly the same as the commercial catalyst with 20 wt.% Pt–Ru.
(5) The catalytic electrode fabricated with 80 wt.% of Pt–Ru/XC or Pt–Ru/MC and 20 wt.% of Pt–Ru/CNT, all containing 20 wt.% of Pt and Ru, obtains higher electro-catalytic activity than the E-TEK catalyst.
(6) The diameter, length, and entanglement of CNTs as well as the particle size, pore size distribution and surface area of the carbon support affect electro-catalyst performance. Further investigation should explore these effects.

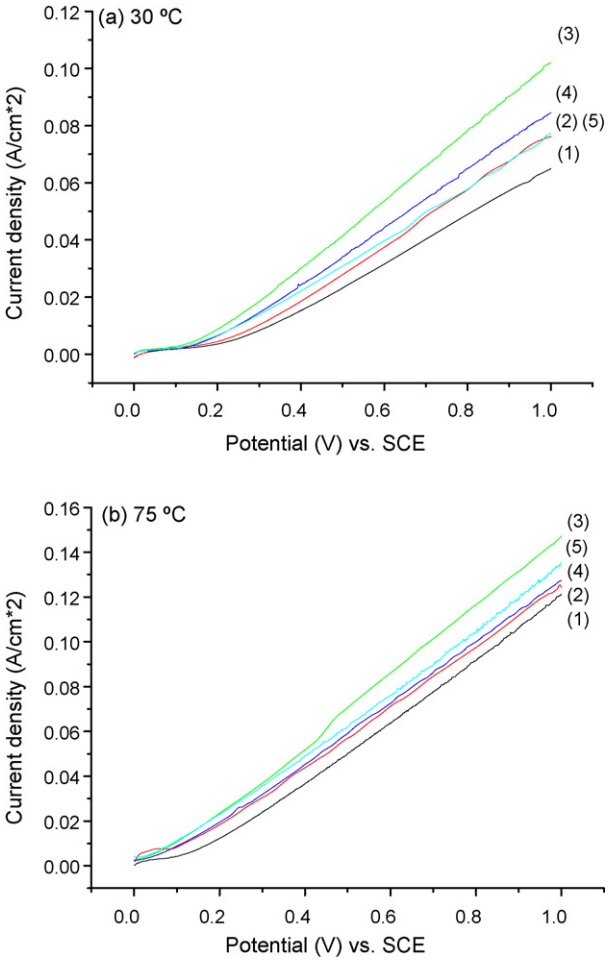

Fig. A1. Comparison of polarization curves with five different types of catalysts: (1) Pt–Ru/XC, (2) Pt–Ru/CNT, (3) Pt–Ru/XC-CNT, (4) mixture of Pt–Ru/XC and Pt–Ru/CNT, and (5) commercial E-TEK.

Acknowledgement

The authors thank the National Science Council of the Republic of China (Taiwan) for financially supporting this research (NSC 94-2623-7-006-012-ET).

Appendix A. A preliminary study on the effect of adding CNTs

In a previous study in our laboratory, XC, CNTs and their mixture were employed as the supports of Pt–Ru catalysts, and the prepared catalysts were used for methanol electro-oxidation. Fig. A1 shows the comparison of polarization curves at 30 and 70 °C with five different types of catalysts: (1) Pt–Ru/XC, (2) Pt–Ru/CNT, (3) Pt–Ru/CNT-XC, (4) mixture of Pt–Ru/XC and Pt–Ru/CNT, and (5) commercial E-TEK. For type (3), Pt–Ru catalyst was deposited after mixing of carbon support of 50 wt.% CNT and 50 wt.% XC. However, type (4) was prepared simply by mixing of 50 wt.% Pt–Ru/CNT and 50 wt.% Pt–Ru/XC. The first four types of catalyst contained 10 wt.% Pt and Ru, and the last type of catalyst contained 20 wt.% Pt and Ru. Apparently, the best performance was obtained from the catalyst Pt and Ru deposited before mixing of the carbon supports among these five types of catalysts. Deposition of metal catalyst Pt and Ru after mixing of catalyst support gave better polarization curve than simply mixing of types (1) and (2). The performance of Pt–Ru/CNT was better than that of Pt–Ru/XC, but not better than that of commercial E-TEK.

References

[1] M. Balddauf, W. Preidel, J. Power Sources 84 (1999) 161.
[2] S.V. Andran, J. Meusinger, J. Power Sources 91 (2000) 193.
[3] M.P. Hogarth, T.R. Ralph, Platinum Met. Rev. 46 (2002) 146.
[4] C. Lamy, A. Lima, V. Le-Rhum, F. Delime, C. Coutanceau, J.-M. Léger, J. Power Sources 105 (2002) 283.
[5] M.M. Markovic, P.N. Ross Jr., Surf. Sci. Reports 45 (2002) 117.
[6] T. Iwasita, Electrochim. Acta 47 (2002) 3663.
[7] A. Kabbabi, R. Faure, R. Durand, B. Beden, F. Hahn, J.-M. Leger, C. Lamy, J. Electroanal. Chem. 444 (1998) 41.
[8] T. Frelink, W. Visscher, J.A.R. van Veen, J. Electroanal. Chem. 382 (1995) 65.
[9] T.C. Deivaraj, J.Y. Lee, J. Power Sources 142 (2005) 43.
[10] J.-H. Wee, K.-Y. Lee, S.-H. Kim, J. Power Sources 165 (2007) 667.
[11] A.L. Dicks, J. Power Sources 156 (2006) 128.
[12] R. Ryoo, S.H. Joo, S. Jun, J. Phys. Chem. B 103 (1999) 7743.
[13] L.A. Solovyov, A.N. Shmakov, V.I. Zaikovskii, S.H. Joo, R. Ryoo, Carbon 40 (2002) 2477.
[14] J. Lee, K. Sohn, T. Hyeon, J. Am. Chem. Soc. 123 (2001) 5146.
[15] M. Carmo, V.A. Paganin, J.M. Rosolen, E.R. Gonzalez, J. Power Sources 142 (2005) 169.
[16] C.L. Lee, Y.C. Ju, P.T. Chou, Y.C. Huang, L.C. Kuo, J.C. Oung, Electrochem. Commun. 7 (2005) 453.
[17] C. Yang, X. Hu, D. Wang, C. Dai, L. Zhang, H. Jin, S. Agathopoulos, J. Power Sources 160 (2006) 187.
[18] Z. He, J. Chen, D. Liu, H. Tamg, W. Deng, Y. Kuang, Mater. Chem. 85 (2004) 396.
[19] Z. He, J. Chen, D. Liu, H. Zhou, Y. Kuang, Diamond Relat. Mater. 13 (2004) (1764).
[20] C.-H. Wang, H.-C. Shih, Y.-T. Tsai, H.-Y. Du, L.-C. Chen, K.-H. Chen, Electrochim. Acta 52 (2006) 1612.
[21] K.I. Han, J.S. Lee, S.O. Park, S.W. Lee, Y.W. Park, H. Kim, Electrochim. Acta 50 (2004) 791.
[22] K.-T. Jeng, C.-C. Chien, N.-Y. Hsu, S.-C. Yen, S.-D. Chiou, S.-H. Lin, W.-M. Huang, J. Power Sources 160 (2006) 97.
[23] M. Gangeri, S. Parathoner, G. Centi, Inorg. Chem. Acta 358 (2006) 4828.